

## Constitutive Modeling for High-Temperature Flow Behavior of W360 Hot Work Tool Steel

Amirarsalani R\* and Morakabati M

Materials Research Center, Malek-Ashtar University of Technology, Iran

### Abstract

In this study, the high-temperature deformation behavior of W360 hot work tool steel was investigated by performing hot compression tests in the temperature range of 900-1200°C at strain rates of 0.001, 0.01, 0.1, and 1 s<sup>-1</sup>. In addition, the flow behavior of the alloy was predicted using constitutive equations by calculating  $\alpha$  from  $\alpha = \beta/n'$  formula and the trial-and-error method. According to the results, the flow behavior of the alloy was different in the range of 900-1000°C and 1000-1200°C due to the presence of carbides at 900°C. The hot deformation activation energy of the alloy in the strain rate range of 0.001-1 s<sup>-1</sup> and each temperature range of 900-1000°C and 1000-1200°C, were obtained to be 641.6 and 434.4 kJ.mol<sup>-1</sup>, respectively. Furthermore, the effect of strain on constitutive equations was investigated through its effect on the deformation constants. Finally, the flow curves were predicted using the hyperbolic sine equation, and compared with the experimental results. The correlation coefficient between the experimental and predicted data in both  $\alpha$  calculation methods was obtained to be 0.998. Also, and the average absolute relative error in  $\alpha$  calculation method from  $\alpha = \beta/n'$  formula and the trial-and-error method was obtained to be 3.47 and 3.25%, respectively. These results indicated the accuracy of the constitutive equations and its ability to explain the deformation behavior of the alloy.

**Keywords:** W360 hot work tool steel; Hot compression; Constitutive equations; Activation energy

### Introduction

A tool steel for dies and punches in warm and hot forging is required to have high hardness/strength to resist wear and deformation, adequate toughness to resist cracking, and retain its hardness at high temperatures in a manner similar to hot work tool steels. All these features were not combined in hot work tool steels such as H10 and H13, which were previously used in hot forging, and they may have worn or deformed relatively quickly so that the tools would soon become out of tolerance. Therefore, a new hot work tool steel named W360 has been developed by Bohler Edelstahl Company. This alloy has the combined advantages of the high hardness of high speed steel with the very good toughness of a hot work tool steel. These are characteristics which can significantly increase the life-time of the tool. Hot working is one of the stages of producing the alloy [1].

W360 tool steel is a medium carbon steel and has about 9% alloying elements. Alloying elements are added to tool steels to improve hardenability, grain growth control, strength, hardness, wear resistance, and their retention at high temperatures. These characteristics are achieved by a combination of solid solution enrichment of the matrix as well as precipitation of the alloy carbides. The microstructural effects of the alloying elements which provide desirable service properties of tool steels make for difficulties in deformation processing. The hard alloy carbides precipitate relatively rapidly on cooling, causing increase in flow stress and decrease in ductility. Deformation is constrained at higher temperatures due to incipient melting of the alloy phases [1-3].

A few researches on this alloy have been carried out by its manufacturing company. In one of these researches [4], the introduction of the alloy and its physical and mechanical properties has been studied. In another work [5] the criteria for selection of die materials that can be used for hot and warm forging of steel in mechanical press with good die life has been suggested. The results indicated that hot work die materials such as Bohler W360, Daido DRM1, and Nachi Duro F1 are better suited than other commercially available hot work tool steels for hot and warm extrusion dies which are subjected to high temperatures.

Furthermore, the hot hardness curves showed that during forging, W360 and DRM1 more retain their hardness (at temperatures above 550°C) compared to other materials.

Bokota et al. [6] have presented the complex hardening model of W360 alloy. Model of estimation of phase fractions and their kinetics was based on the continuous heating (CHT) and continuous cooling (CCT) diagrams. The volume fraction of phases which form during the continuous heating and cooling (austenite, pearlite or bainite) are described by Johnson-Mehl (JM) formula. The result showed that the alloy is hardened very easy and the cooling rate must be lower than 3.2 K.s<sup>-1</sup> to obtain the bainite-martensite structure.

In addition to microstructure, processing parameters such as temperature, strain, and strain rate also play an important role in hot deformation of the alloy as a critical stage of its production. Flow behavior of materials during hot deformation processes is a complicated phenomenon. Understanding of metal flow pattern and kinetic of metallurgical processes under hot deformation conditions is very important for engineers in metal forming industries. Simulation of flow behavior by modeling methods has an important effect on time and cost saving. Modeling the flow behavior is done by determining the appropriate constitutive equations that interact the flow stress with strain, temperature, and strain rate. Therefore, a number of researchers [7,8] have attempted to develop material constitutive equations from experimentally measured data in order to describe hot

\*Corresponding author: Amirarsalani R, Materials Research Center, Malek-Ashtar University of Technology, Iran, Tel: +98 21 2294 5140; E-mail: ramirarsalani1992@gmail.com

Received November 12, 2018; Accepted November 28, 2018; Published December 08, 2018

Citation: Amirarsalani R, Morakabati M (2018) Constitutive Modeling for High-Temperature Flow Behavior of W360 Hot Work Tool Steel. J Material Sci Eng 7: 497. doi: 10.4172/2169-0022.1000497

Copyright: © 2018 Amirarsalani R, et al. This is an open-access article distributed under the terms of the Creative Commons Attribution License, which permits unrestricted use, distribution, and reproduction in any medium, provided the original author and source are credited.

deformation behavior. Hot compression test is the most common test for extrapolation of the constitutive equations. On the other hand, lack of information in the hot deformation behavior of W360 hot work tool steel is available. Therefore, the purpose of this study is to model the flow behavior of the alloy and predict the true stress-true strain curves by means of hot compression test.

## Materials and Methods

In this work, the W360 hot work tool steel was melted in the induction furnace under argon gas and then cast in metal mould. The electroslag remelting (ESR) process was then performed. The chemical composition of the manufactured alloy is given in Table 1.

The ingot after homogenization for 4 h at 1150°C, was annealed for 4 h at 800°C according to the reference to softening and prevent cracking and increase in its deformability [9]. The ingot was then rolled at 1150°C to a thickness reduction of 67%. Then, the belt was annealed for 3 h at 850°C to increase machinability. The cylindrical hot compression test specimens were machined to 8 mm diameter and 12 mm length (according to ASTM E209 [10] with keeping aspect ratio). The test specimens were cut along perpendicular to the direction of rolling by the wire cut machine. A thin layer of graphite was rubbed on contacting surface to minimize friction between the specimen and the anvils. Uniaxial hot compression tests were performed by an Instron 8502 testing machine that equipped with resistant furnace. A thin layer of graphite was rubbed on contacting surface to minimize friction between the specimen and the anvils. To allow thermal homogenization, the specimens were hold in the test temperature for 10 minutes. The specimens were deformed with 100°C intervals in the temperature range of 900-1200°C at strain rates of 0.001, 0.01, 0.1, and 1 s<sup>-1</sup>. The specimens were deformed up to total strain of 0.7. At the end of the test the specimens were withdrawn from the furnace quickly and water quenched to preserve the as-worked microstructure. In order to examine microstructure, sections of deformed specimens

were cut parallel to compression axis and were prepared by standard metallographic techniques and were then etched in 4 pct nital etchant. Observations of microstructure were carried out using an Olympus BX 51 optical microscopy. Also, SEM images were prepared using a VEGA II TESCAN scanner electron microscope with a working voltage of 20 kV and equipped with an EDS analyzer and the results were then analyzed and evaluated.

## Results and Discussion

The optical and scanning electron microscopic images of the alloy in the rolled and annealed condition are presented in Figure 1a and 1b. Average grain size of initial microstructure was determined to be 53 ± 5 μm. According to Figure 1b, the alloy consists of particles that their volume fraction were estimated to be about 5.1%. Figure 1c shows a linear analysis of the particles. According to this figure, the existing particles are carbides and they are similar to molybdenum-rich carbides.

The true stress-true strain curves of the alloy derived from hot compression tests at various strain rates and temperatures are presented in Figure 2. At the beginning of deformation, with increasing strain, the stress increases linearly to the yield point. Afterwards, with increase in strain and entrance to the plastic zone, the dislocations density increases and work hardening occurs. It has been reported [11,12] that, due to the low stacking fault energy of tool steels, climb and cross slip are inhibited thus diminishing the amount of recovery. As the dislocation substructure becomes denser and more inhomogeneous, in a critical strain (ε<sub>c</sub>), the driving force is attained for new grains to nucleate, predominantly at the boundaries of existing grains.

The flow stress dependence on temperature and strain rate is generally given by a functional form that incorporates the Zener-Hollomon parameter [13-15]. As shown in Figure 2, the flow stress levels were reduced by increasing temperature and decreasing strain rate. The

Fe	Cr	Mo	V	C	Mn	Si	P	S
Bal.	5.30	2.69	0.52	0.48	0.71	0.27	0.01	0.008

Table 1: Chemical composition of the used W360 hot work tool steel after ESR (wt.%).

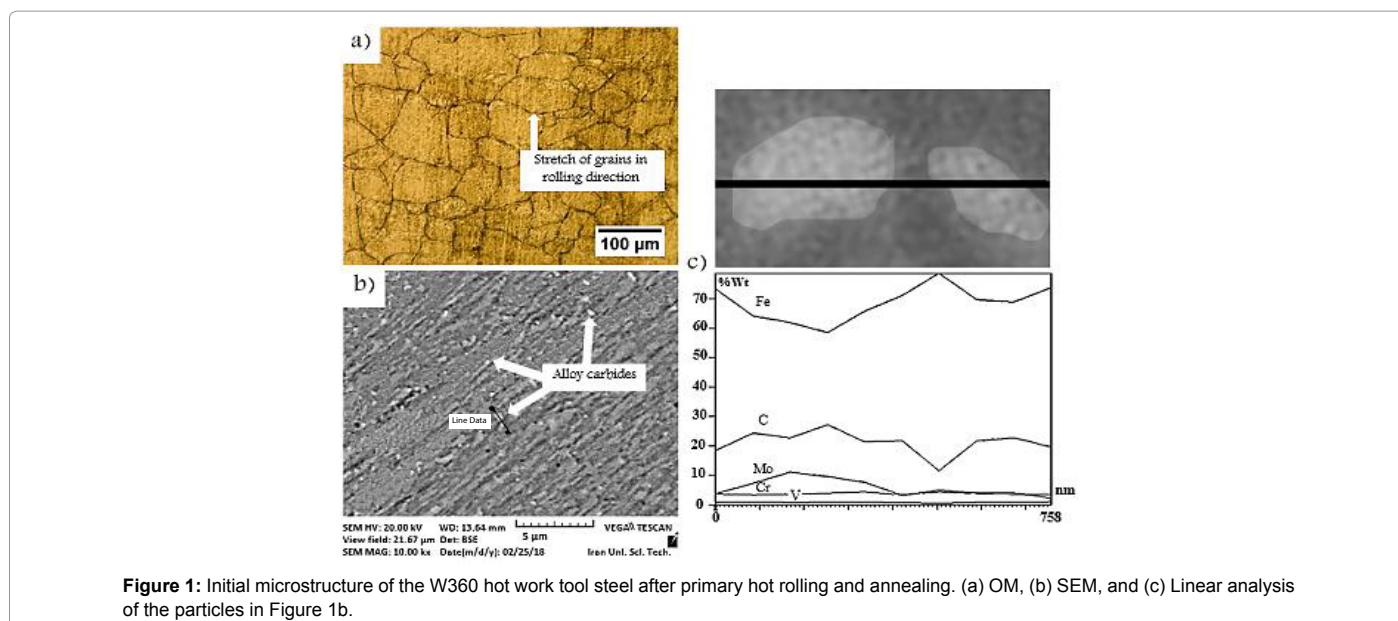
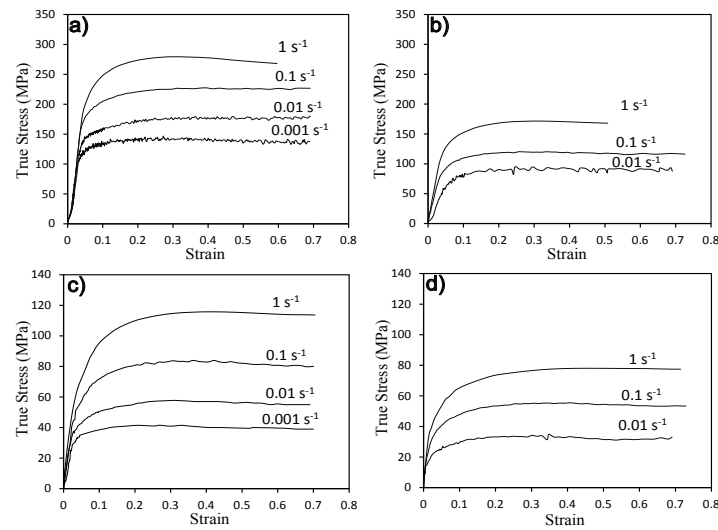


Figure 1: Initial microstructure of the W360 hot work tool steel after primary hot rolling and annealing. (a) OM, (b) SEM, and (c) Linear analysis of the particles in Figure 1b.



**Figure 2:** True stress-true strain curves of the W360 alloy derived from hot compression tests at various strain rates at temperatures of (a) 900°C, (b) 1000°C, (c) 1100°C, and (d) 1200°C.

cause lies in the fact that the lower strain rate and higher temperature provide longer time for the energy accumulation and higher mobility at boundaries which result in the nucleation and growth of dynamically recrystallized grains and dislocation annihilation [16]. In contrast, the strength levels increase significantly with decreasing temperature and increasing strain rate.

Constitutive equations can be determined by using the flow curves data. Flow curves can be predicted at different temperatures and strain rates using constitutive equations. To characterize the deformation behavior of each material, it is necessary to determine its deformation constants such as activation energy by using Zener-Hollomon parameter according to eqn. (1) [17]. In this equation,  $f(\sigma)$  is the stress function that can be calculated by the power law (eqn. (2)), exponential (eqn. (3)), and hyperbolic sine (eqn. (4)) functions [3,14]:

$$Z = \dot{\epsilon} \exp\left(\frac{Q}{RT}\right) = f(\sigma) \quad (1)$$

$$z = f(\sigma) = A' \sigma^n \quad , \text{ for } \alpha_\sigma < 0.8 \quad (2)$$

$$z = f(\sigma) = A'' \exp(\beta \sigma) \quad , \text{ for } \alpha_\sigma > 1.2 \quad (3)$$

$$z = f(\sigma) = A[\sinh(\alpha \sigma)]^n \quad (4)$$

In which  $Z$  is Zener-Hollomon parameter ( $s^{-1}$ ),  $\dot{\epsilon}$  is strain rate ( $s^{-1}$ ),  $T$  is temperature (K),  $R$  is universal gas constant ( $8.314 \text{ J} \cdot \text{mol}^{-1} \cdot \text{K}^{-1}$ ),  $Q$  is activation energy ( $\text{J} \cdot \text{mol}^{-1}$ ),  $\sigma$  is flow stress (Pa), and  $A, A', A'', n, \alpha,$  and  $\beta$  are material's constants.

At relatively low stress values (i.e.  $\alpha \sigma < 0.8$ ) the power law is usually used to model deformation behavior of materials (eqn. (2)). On the other hand, the exponential equation (eqn. (3)) is more favorable than power law to model hot working conditions at higher stresses (i.e.  $\alpha \sigma > 0.8$ ) [3,14]. This is while the hyperbolic sine law can be applied for a wide range of stress levels. Therefore, the hyperbolic sine law is generally preferred to the exponential and power law. However, the first two equations (eqns. (2) and (3)) are commonly used in order to extract  $\beta$  and  $n'$  and then calculate  $\alpha$  according to  $\alpha = \beta/n'$  formula [7]. Eqns. (5)-(7) can be obtained by substituting eqn. (1) into eqns. (2)-(4) and then taking the natural logarithm from both sides in equations [14,18].

$$\ln \dot{\epsilon} = n' \ln \sigma - \frac{Q}{RT} + \ln A' \quad (5)$$

$$\ln \dot{\epsilon} = \beta \sigma - \frac{Q}{RT} + \ln A'' \quad (6)$$

$$\ln \dot{\epsilon} = n \ln [\sinh(\alpha \sigma)] - \frac{Q}{RT} + \ln A \quad (7)$$

The values of  $n'$  and  $\beta$  can be obtained from the mean slope of  $\ln \dot{\epsilon} - \ln \sigma$  and  $\ln \dot{\epsilon} - \sigma$  plots at constant temperatures, respectively (Figure 3). The mean values of  $n'$  and  $\beta$  were calculated to be 7.48 and  $0.075 \text{ MPa}^{-1}$ , respectively. The value of  $\alpha$  was obtained to be  $0.01 \text{ MPa}^{-1}$  by substituting the  $n'$  and  $\beta$  values in the  $\alpha = \beta/n'$  formula.

The trial-and-error is another way for  $\alpha$  determination. In this method, a value of  $\alpha$  is estimated as a first approximation and then, the accuracy of the chosen value is evaluated by plotting  $\ln [\sinh(\alpha \sigma)]$  vs  $1/T$ . The  $\alpha$ -value is chosen in a way that parallel lines will be obtained in each strain rate [18]. In this condition, it can be expected that the alloy's flow behavior will be calculated more accurately. Thus, the results of modeling with  $\alpha$  parameter which were extracted by trial-and-error method will be presented in the following. Finally, the results of predicted flow stress by both of  $\alpha$ -values were expressed and compared. By this method, the best value of  $\alpha$  was determined to be  $0.008 \text{ MPa}^{-1}$ . By substituting the  $\alpha$ -value into eqn. (7) and through plotting the graph of  $\ln \dot{\epsilon} - \ln [\sinh(\alpha \sigma)]$  at constant temperatures (Figure 4a), and calculating the mean slope, the value of  $n$  was determined to be 5.64. At constant strain rate, the partial differentiation of eqn. (7) leads to the following equation:

$$Q = Rn \left[ \frac{\partial \ln [\sinh(\alpha \sigma_p)]}{\partial \left(\frac{1}{T}\right)} \right]_{\dot{\epsilon}} \quad (8)$$

By plotting the  $\ln [\sinh(\alpha \sigma)]$  vs  $1/T$  at constant strain rate as shown in Figure 4b, and calculating the mean slope, the hot deformation activation energy ( $Q$ ) was determined to be  $514.5 \text{ kJ} \cdot \text{mol}^{-1}$ . This value for the  $Q$  was compared with other investigations according to Table 2. The results showed that the obtained activation energy is more than of

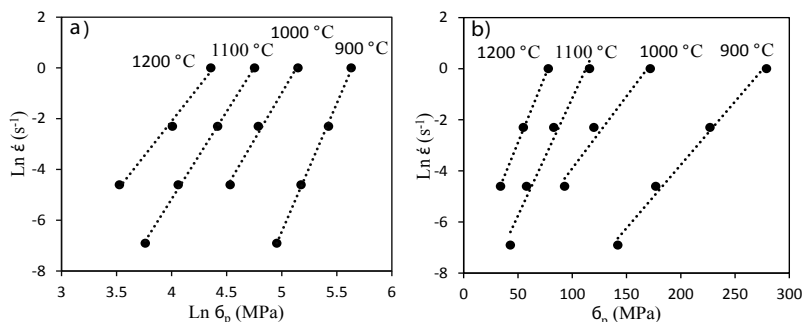


Figure 3: Graphs of  $\ln \dot{\epsilon}$  vs (a)  $\ln \sigma_p$ , and (b)  $\sigma_p$ .

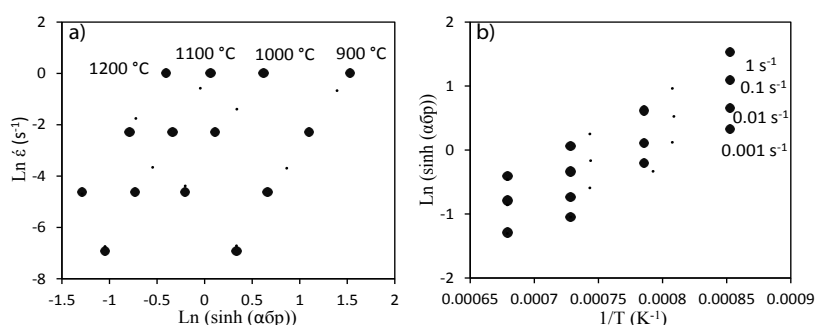


Figure 4: Graphs of (a)  $\ln \dot{\epsilon}$  vs.  $\ln (\sinh (\alpha \sigma_p))$ , and (b)  $\ln (\sinh (\alpha \sigma_p))$  vs.  $1/T$ .

Steel	Compositions	Q (kJ.mol <sup>-1</sup> .K <sup>-1</sup> )	Reference
H13	0.39C-5.29Cr-1.35Mo-1.02Si-0.6Mn-0.83V	444	[21]
H13	0.4C-5Cr-1Mo-1V	424	[22]
M2	0.8C-6W-5Mo-4Cr-2V	438	[22]
A2	0.99C-4.95Cr-0.94Cr-0.48Mn-0.18V	400	[23]
W360	0.48C-5.3Cr-2.69Mo-0.27Si-0.71Mn-0.52V	514.5	Present work

Table 2: The calculated activation energy (Q) for selected tool steels.

the reported values in the references. In a work that the flow behavior of H13 tool steel has been studied [2], it has been shown that, in the  $\sigma$  vs  $1/T$  plots, slope changing was observed with decreasing temperature from 1000 to 900°C, and by considering the exponential equation in the whole range of 900 to 1100°C, the amount of Q was obtained very high, while more reasonable value of Q was obtained in the range of 1000 to 1100°C. On the other hand, a number of researchers have reported [2,19,20] that if a new hardening or softening mechanism, such as precipitation or modification of texture, begins to operate under some deformation conditions, the value of the apparent activation energy also changes. Hence, requiring the determination of new values for the parameters of constitute Equations. In the present study, changing the slope of  $\ln (\sinh (\alpha \sigma_p))$  vs  $1/T$  plots, were observed with decreasing temperature from 1000 to 900°C, too. Therefore, the graph of  $\ln (\sinh (\alpha \sigma_p))$  vs  $1/T$  for the alloy was re-plotted and the slope changes are shown in Figure 5. The dashed lines in the graphs were drawn to eliminate the effect of strength increasing at 900°C.

According to eqn. (4), the constant value of A can be obtained from the intercept of the  $\ln Z$ - $\ln (\sinh (\alpha \sigma_p))$  graph. The values of n, Q, and  $\ln A$  calculated in each temperature range of 900 to 1000°C, 1000 to 1200°C, and 900 to 1200°C are summarized in Table 3.

The optical micrographs of the alloy after deformation at the strain

rate of 0.1 s<sup>-1</sup>, and temperatures of 900 and 1000°C are shown in Figure 6. From this figure it can be seen that due to the occurrence of dynamic recrystallization, a fine-grained microstructure was obtained with increasing temperature from 900 to 1000°C. In addition, according to the study about H13 hot work tool steel [2], with increasing temperature from 900 to 1000°C, the volume fraction of carbides decreased from 10 to 1.3%. Therefore, the solubility of alloy carbides and the occurrence of dynamic recrystallization can simultaneously reduce the activation energy at temperatures above 1000°C compared to temperatures less than 1000°C.

By considering the activation energy in the range of 900 to 1200°C, the peak stress at 800°C, and 1 s<sup>-1</sup> would be 363 MPa for the alloy. Such an extrapolation may not match reality since as reported in the reference [2], the effect of alloy carbides precipitation would be relatively less significant between 900 and 800°C compared to a temperature drop of 1000 to 900°C. In addition, as reported in the reference [1], the alloy transforms from austenite to ferrite at about 860°C upon equilibrium cooling. Therefore, due to the softening of ferrite, the expected strength for it at this temperature is less than 363 MPa. Therefore, according to Table 3, the amount of activation energy of the alloy in the range of 1000 to 1200°C was obtained to be 443.4 kJ.mol<sup>-1</sup>. This value is approximately equal to the amount of activation energy reported by Ryan et al. [21,22], according to Table 2, for H13 hot work tool steel (444 kJ.mol<sup>-1</sup>).

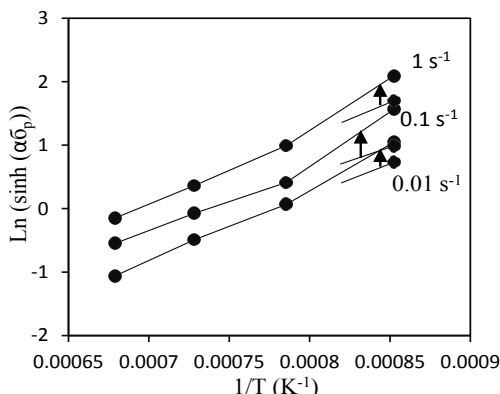


Figure 5: Graph of Ln (sinh (ασ<sub>p</sub>)) vs. 1/T at different strain rates to show the slope change occurred at 900°C.

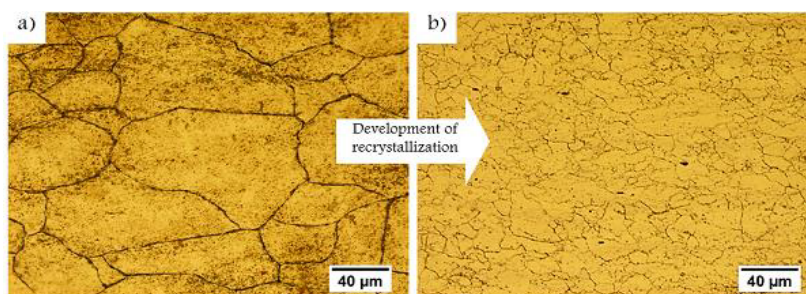


Figure 6: W360 tool steel microstructures after deformation at the strain rate of 0.1 s<sup>-1</sup>, and at temperatures of (a) 900°C, and (b) 1000°C.

Deformation temperature range (°C)	Q (kJ.mol <sup>-1</sup> )	n	Ln A
900-1200	514.5	5.64	44.57
900-1000	641.6	5.61	57.31
1000-1200	443.4	5.68	38.51

Table 3: n and Q values calculated for W360 tool steel in various temperature ranges.

The strain influence is neglected in eqns. (5) to (7) [23]. However, according to Figure 2, the values of stress, deformation activation energy, and other material constants were strongly influenced by the strain. Therefore, in order to predict the flow curves, Q and other material constants were evaluated at 0.05 intervals in strain range of 0.1-0.7 using the aforementioned methods and the constitutive equations were then calculated. The changing constants with strain are shown in Figure 7.

A 5th order polynomial equations, as shown in eqn. (9), were found to represent the influence of strain on material constants with very good correlation and generalization. Also, the coefficients of the polynomial functions are given in Table 4.

$$Y = B_0 + B_1\varepsilon^1 + B_2\varepsilon^2 + B_3\varepsilon^3 + B_4\varepsilon^4 + B_5\varepsilon^5 \quad (9)$$

By taking the natural logarithm of the sides of eqn. (4), flow stress can be written as a function of the Zener-Hollomon parameter, as shown in eqn. (10).

$$\sigma = \frac{1}{\alpha} \ln \left\{ \left( \frac{Z}{A} \right)^{1/n} + \left[ \left( \frac{Z}{A} \right)^{2/n} + 1 \right]^{1/2} \right\} \quad (10)$$

The constitutive equations were calculated at different strains by substituting the calculated deformation constants (Table 4) in eqn. 10, and the true stress-true strain curves of the alloy were predicted at 1000

and 1200°C, at strain rate of 0.001 s<sup>-1</sup>, in which hot compression test were not performed. The graph of peak stress vs temperature at various strain rates is shown in Figure 8 (the hollow circular points in these graphs, show the predicted peak stress at the strain rate of 0.001 s<sup>-1</sup> at temperatures of 1000 and 1200°C). The results of the prediction showed a proper trend with temperature and strain rate. Similarly, it is possible to predict the flow curves at different temperatures and strain rates by means of the proposed equation, without carrying out experiments. It helps us to save both the time and cost of the experiments.

In order to evaluate the proposed equations for predicting alloy behavior and also, to compare the method of a estimation with the method of its calculation through the α=β/n' formula, the predicted stress-strain curves (solid lines) compared with the experimental ones (dots) are shown in Figure 9.

In these graphs, there is a good conformity between the experimental and predicted data by two methods. Also, the correlation between the experimental and predicted flow stress data under different deformation temperatures and strain rates are shown in Figure 9. In this figure dashed lines show the best possible conditions for predicting the flow stress, in which the predicted stress will be equal to the experimental stress. According to this figure, the approach of the data to each other and the best linear regression is excellent in the both methods.

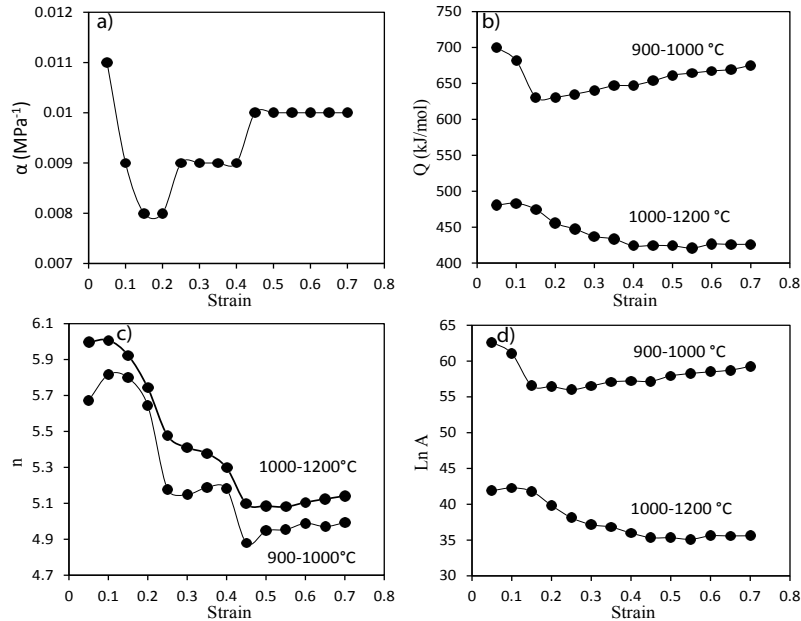


Figure 7: Graphs of the W360 alloy constitutive equations parameters, (a)  $\alpha$ , (b)  $Q$ , (c)  $n$ , and (d)  $\ln A$  vs. strain in each temperature range.

Parameter	Temperature range (°C)	$B_0$	$B_1$	$B_2$	$B_3$	$B_4$	$B_5$
Q	900-1200	0.01511	-1.10978	0.61577	-1.52704	1.78787	-0.80654
	900-1000	764.25515	-1432.5059	5158.16337	-6676.11454	1812.29626	1437.14001
	1000-1200	464.49429	574.27058	-5390.00688	15464/8152	-18845.1671	8459.40411
n	900-1000	5.07216	18.2058	-141.42615	406.77385	-517.33411	245.02628
	1000-1200	5.83425	5.95713	-56.97096	158.04996	-191.3543	88.05917
Ln A	900-1000	67.73798	-108.56336	306.91983	-162.97177	-381.27628	384.65984
	1000-1200	39.28844	83.87223	-711.47505	1988.3102	-2403.27885	1079.00929

Table 4: Polynomial fitting results of  $\alpha$ ,  $n$ ,  $Q$ , and  $\ln A$  of the W360 alloy.

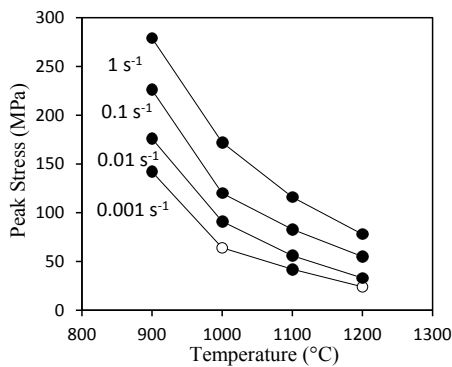


Figure 8: Graph of peak stress vs. temperature at different strain rates.

The accuracy of the constitutive equation is also further assessed using standard statistical parameters such as correlation coefficient ( $R$ ) and average absolute relative error (AARE). They are expressed as [24]:

$$R = \frac{\sum_{i=1}^n (E_i - \bar{E})(P_i - \bar{P})}{\sqrt{\sum_{i=1}^n (E_i - \bar{E})^2 \sum_{i=1}^n (P_i - \bar{P})^2}} \quad (11)$$

$$AARE = \frac{1}{n} \sum_{i=1}^n \left| \frac{E_i - P_i}{E_i} \right| \times 100 \quad (12)$$

Method of $\alpha$ calculation	R	AARE%
$\alpha = \beta/n'$	0.998	3.47
Trial-and-error	0.998	3.25

Table 5: Comparison of the  $R$  and AARE% between the experimental and predicted data obtained by calculating  $\alpha$  from  $\alpha = \beta/n'$  formula and the trial-and-error method.

Where  $E_i$  is the experimental flow stress,  $P_i$  is the predicted flow stress derived from the developed constitutive equation at  $i$ th strain,  $\bar{E}$  and  $\bar{P}$  are the mean values of  $E$  and  $P$ , respectively, and  $n$  is the total number of data which are employed in this work. Ideal modeling occurs when  $R=1$  and  $AARE=0\%$ . The correlation coefficient is used to reflect the capability of the linear relationship between the experimental and predicted data. The AARE is also computed through a term-by-term comparison of the relative error and therefore, it is an unbiased statistical parameter to measure the predictability of a model/equation. Table 5 shows the comparison of the  $R$  and AARE% between the experimental and predicted data obtained by calculating  $\alpha$  from  $\alpha = \beta/n'$  formula and the trial-and-error method.

The obtained values of  $R$  and AARE% from both methods reflect the excellent predictability of the developed constitutive equations. Since the hot deformation parameters (temperature and strain rate) appear in the constitutive equation through the Zener-Holloman parameter, the flow curves behavior at all temperatures and strain rates can be predicted well.

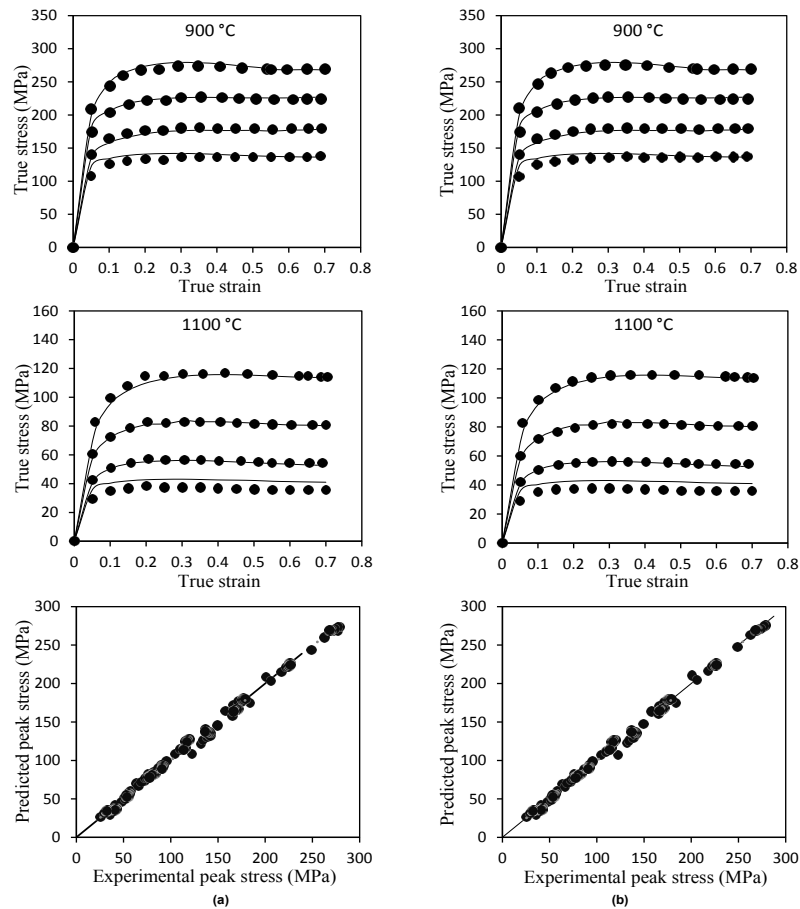


**Figure 9:** Comparison between the results of experimental and predicted flow stress obtained from the Arrhenius-type constitutive equation that  $\alpha$  was calculated using (a)  $\alpha=\beta/n'$  formula, and (b) trial-and-error method.

## Conclusion

The hot deformation behavior of W360 hot work tool steel has been investigated over a wide range of temperatures (900-1200°C) and strain rates (0.001-1 s<sup>-1</sup>) by performing isothermal hot compression tests. The significant results presented in the paper can be summarized as follows:

- According to the flow curves, with increasing temperature and decreasing strain rate, the flow curves dropped and the strength decreased due to increase in softening time and mobility at boundaries which result in the nucleation and growth of dynamically recrystallized grains and dislocation annihilation.
- Due to the low SFE of the alloy, a significant degree of recrystallization has been occurred at 1000°C and strain rate of 1 s<sup>-1</sup>. The occurrence of dynamic recrystallization and dissolution of carbides at 1000°C simultaneously reduced the activation energy at temperatures above 1000°C compared to temperatures less than 1000°C.
- The hot deformation activation energy of the alloy in the strain rate range of 0.001-1 s<sup>-1</sup> and each ranges of 900-1000°C and 1000-1200°C, were obtained to be 641.6 and 434.4 kJ.mol<sup>-1</sup>, respectively.
- Two hyperbolic sine equations were presented in each

range of 900-1000°C and 1000-1200°C for modeling the hot deformation behavior of the alloy and the stress-strain curves were then predicted.

- The influence of strain in the constitutive equation was incorporated by considering the influence of strain on material constants (i.e.  $\alpha$ ,  $n$ ,  $Q$ , and  $\ln A$ ). The results showed that the constants of the material depend strongly on the strain.
- In order to predict the flow behavior of the alloy, two methods were used for calculating  $\alpha$ . They are  $\alpha=\beta/n'$  formula and the trial-and-error method. The correlation coefficient between the experimental and predicted data in both  $\alpha$  calculation methods was obtained to be 0.998 and average absolute relative error of the methods of calculating  $\alpha$  from  $\alpha=\beta/n'$  formula and the trial-and-error method was obtained to be 3.47 and 3.25%, respectively. It indicates the accuracy of the constitutive equations and their ability to explain the hot deformation behavior of the alloy.

## References

1. Schweiger KH, Asenberger JH, Dremel H (2002) New tool steel for warm and hot forging. Proceedings of the International Tooling Conference, Karlstad, Sweden pp: 129-139.
2. Imbert C, Ryan ND, McQueen HJ (1984) Hot workability of three grades of tool steel. Metallurgical Transactions A 15: 1855-1864.

3. Imbert C, McQueen H (2001) Peak strength, strain hardening and dynamic restoration of A2 and M2 tool steels in hot deformation. *Mater Sci Eng A* 313: 88-103.
4. Lin YC, Li KK, Li HB, Chen J, Chen XM, et al. (2015) New constitutive model for high-temperature deformation behavior of inconel 718 superalloy. *Materials and Design* 74: 108-118.
5. Altan T, Deshpande M (2011) Selection of die materials and surface treatments for increasing die life in hot and warm forging. ERC for Net Shape Forming, Proceedings of the FIATECH Technology Conference & Showcase.
6. Bokota A, Kulawik A, Szymczyk R, Wróbel J (2015) The Numerical Analysis of the Phenomena of Superficial Hardening of the Hot-Work Tool Steel Elements. *Archives of Metallurgy and Materials* 60: 2763-2772.
7. Sanrutsadakorn A, Uthaisangsuk V, Suranuntchai S, Thossatheppitak B (2013) Constitutive modeling of flow behaviour of AISI 4340 steel under hot working conditions. *Applied Mechanics and Materials* 249: 863-869.
8. Lin YC, Chen XM (2011) A critical review of experimental results and constitutive descriptions for metals and alloys in hot working. *Materials & Design* 32: 1733-1759.
9. Davis JR (Ed) (1995) ASM specialty handbook: tool materials. ASM International.
10. ASTM E209 (2010) Standard practice for compression tests of metallic materials at elevated temperatures with conventional or rapid heating rates and strain rates. ASTM International.
11. Ezatpour HR, Sajjadi SA, Haddad-Sabzevar M, Ebrahimi GR (2012) Hot deformation and processing maps of K310 cold work tool steel. *Materials Science and Engineering A* 550: 152-159.
12. Imbert C, McQueen H (2001) Dynamic recrystallization of A2 and M2 tool steels. *Materials Science and Engineering A* 313: 104-116.
13. Dieter GE, Kuhn HA, Semiatin SL (2013) Handbook of workability and process design. ASM International.
14. Yang H, Li Zh, Zhang ZI (2006) Investigation on Zener-Hollomon parameter in the warm-hot deformation behavior of 20CrMnTi. *Journal of Zhejiang University-Science A* 7: 1453-1460.
15. McQueen H, Imbert C (2004) Dynamic recrystallization: plasticity enhancing structural development. *Journal of Alloys and Compounds* 378: 35-43.
16. Quan GZ, Li GS, Chen T, Wang YX, Zhang YW, et al. (2011) Dynamic recrystallization kinetics of 42CrMo steel during compression at different temperatures and strain rates. *Materials Science and Engineering A* 528: 4643-4651.
17. Sellars CM, Tegart WJM (1972) Hot Workability. *International Metallurgical Reviews* 17: 1-24.
18. Rokni MR, Zarei-Hanzaki A, Roostaei A, Abolhasani A (2011) Constitutive base analysis of a 7075 aluminum alloy during hot compression testing. *Materials & Design* 32: 4955-4960.
19. Balancin O, Hoffmann W, Jonas JJ (2000) Influence of microstructure on the flow behavior of duplex stainless steels at high temperatures. *Metallurgical and materials transactions A* 31: 1353-1364.
20. Junior J, Moreira A, Balancin O (2005) Prediction of steel flow stresses under hot working conditions. *Materials research* 8: 309-315.
21. Ryan N, McQueen H (1986) Mean pass flow stresses and interpass softening in multistage processing of carbon-, HfSA-, tool- and  $\gamma$ -stainless steels. *Journal of mechanical working technology* 12: 323-349.
22. Ryan ND, McQueen HJ (1986) Effects of alloying upon the hot workability of carbon, microalloyed, tool, and austenitic stainless steels. *Journal of mechanical working technology* 12: 279-296.
23. Li HY, Li YH, Wei DD, Liu JJ, Wang XF (2011) Constitutive equation to predict elevated temperature flow stress of V150 grade oil casing steel. *Materials Science and Engineering A* 530: 367-372.
24. Mohamadizadeh A, Zarei-Hanzaki A, Abedi HR (2016) Modified constitutive analysis and activation energy evolution of a low-density steel considering the effects of deformation parameters. *Mechanics of Materials* 95: 60-70.